Biomaterials 33 (2012) 4379–4391

Contents lists available at SciVerse ScienceDirect

Biomaterials

journal homepage: www.elsevier.com/locate/biomaterials

Surface modified magnetic nanoparticles for immuno-gene therapy of murine mammary adenocarcinoma

Sara Prijic [a,1], Lara Prosen [a,1], Maja Cemazar [b,g], Janez Scancar [c], Rok Romih [d], Jaka Lavrencak [e], Vladimir B. Bregar [f], Andrej Coer [g], Mojca Krzan [h], Andrej Znidarsic [a], Gregor Sersa [b,*]

[a] Kolektor Group, Nanotesla Institute, Ljubljana, Slovenia
[b] Institute of Oncology Ljubljana, Department of Experimental Oncology, Ljubljana, Slovenia
[c] Josef Stefan Institute, Department of Environmental Sciences, Ljubljana, Slovenia
[d] University of Ljubljana, Faculty of Medicine, Institute of Cell Biology, Ljubljana, Slovenia
[e] Institute of Oncology Ljubljana, Department of Cytopathology, Ljubljana, Slovenia
[f] Kolektor Group, Kolektor Magma, Ljubljana, Slovenia
[g] University of Primorska, Faculty of Health Sciences, Izola, Slovenia
[h] University of Ljubljana, Faculty of Medicine, Institute of Pharmacology and Experimental Toxicology, Ljubljana, Slovenia

ARTICLE INFO

Article history:
Received 30 January 2012
Accepted 16 February 2012
Available online 18 March 2012

Keywords:
Nanoparticles
Gene therapy
Cytokine
Polyacrylic acid
Magnetism
Gene transfer

ABSTRACT

Cancer immuno-gene therapy is an introduction of nucleic acids encoding immunostimulatory proteins, such as cytokine interleukin 12 (IL-12), into somatic cells to stimulate an immune response against a tumor. Various methods can be used for the introduction of nucleic acids into cells; magnetofection involves binding of nucleic acids to magnetic nanoparticles with subsequent exposure to an external magnetic field. Here we show that surface modified superparamagnetic iron oxide nanoparticles (SPIONs) with a combination of polyacrylic acid (PAA) and polyethylenimine (PEI) (SPIONs-PAA-PEI) proved to be safe and effective for magnetofection of cells and tumors in mice. Magnetofection of cells with plasmid DNA encoding reporter gene using SPIONs-PAA-PEI was superior in transfection efficiency to commercially available SPIONs. Magnetofection of murine mammary adenocarcinoma with plasmid DNA encoding IL-12 using SPIONs-PAA-PEI resulted in significant antitumor effect and could be further refined for cancer immuno-gene therapy.

1. Introduction

The translation of nanotechnology has already widespread into biomedicine for diagnostic, therapeutic and theranostic purposes [1]. Superparamagnetic iron oxide nanoparticles (SPIONs) can be guided by an external magnetic field, yet due to quantum effects at the nanometer scale they do not retain residual magnetism in the absence of an external magnetic field [2], which makes them especially suitable for diverse biomedical applications [3]. In the field of oncology, SPIONs have been exploited for diagnostic purposes as contrast enhancers for magnetic resonance imaging and as vehicles for biomarkers detection [4]. For therapeutic purposes SPIONs have been used for isolation and transfection of hematopoietic stem cells for gene therapy – magselectofection [5], in magnetic hyperthermia [6] and as delivery systems for different therapeutics [7].

Magnetofection is a non-viral transfection method that uses an external magnetic field to target cells with nucleic acids that are bound to magnetic nanoparticles [8]. Magnetofection has recently celebrated its 10th anniversary, and its progress and prospects are described in the thorough review paper [9]. Many studies regarding magnetofection have used commercially available SPIONs [8,10–18]. The majority were coated and/or functionalized with positively charged PEI due to its electrostatic interaction with negatively charged sugar phosphate backbone of nucleic acid and proton sponge effect, which enables release of SPIONs-PEI-nucleic acid complexes from endolysosomes into cytoplasm. Although PEI is a transfection agent *per se* [19], it has been shown that when coupled with SPIONs, magnetofection efficiency increased in comparison to the transfection efficacy of PEI only [11,20]. Despite of its extended usage for gene delivery, PEI compromises cell membrane integrity and induces formation of channels in the outer mitochondrial membrane [21], which could lead to cell death.

* Corresponding author.
E-mail address: gsersa@onko-i.si (G. Sersa).
[1] Authors contributed equally to this work.

0142-9612
doi:10.1016/j.biomaterials.2012.02.061

Similar to PEI, poly(alkylacrylic acid) polymers, including non-cytotoxic polyacrylic acid (PAA), have been considered as endosomolytic polymers [22]. It has been shown that the inclusion of PAA to PEI-DNA transfection complexes not only increased reporter gene expression but also reduced toxicity *in vivo* [23]. However, there are no reports about SPIONs coated with anionic PAA and functionalized with cationic PEI for magnetofection of plasmid DNA encoding either reporter or therapeutic genes. Thus far magnetofection of tumors using SPIONs for magnetically-guided immunogene therapy has not resulted in significant antitumor effect [14,16].

In terms of preparing effective magnetically-guided delivery system for immuno-gene therapy of tumors, we modified surface of SPIONs with a double layer of PAA and PEI endosomolytic polymers (SPIONs-PAA-PEI). After evaluating physicochemical properties and binding plasmid DNA encoding either reporter gene for enhanced green fluorescent protein (GFP) (pDNA^{GFP}) or therapeutic gene for murine interleukin 12 (IL-12) (pDNA^{IL-12}) to SPIONs-PAA-PEI, we tested cytotoxicity of so prepared SPIONs-PAA-PEI-pDNA^{GFP}. We implemented magnetofection of cells of different cell lines with pDNA^{GFP} or pDNA^{IL-12} using SPIONs-PAA-PEI, and we compared its efficacy to transfection efficacy using commercially available magnetic nanoparticles and two well-established non-viral transfection methods, electroporation and lipofection. *In vivo*, we determined acute toxicity and biodistribution of SPIONs-PAA and SPIONs-PAA-PEI-pDNA^{GFP}, and tested non-invasive magnetofection of murine melanoma and mammary adenocarcinoma with pDNA^{GFP} using SPIONs-PAA-PEI. For the proof-of-principle, we determined antitumor effectiveness after magnetofection of murine mammary adenocarcinoma tumors with pDNA^{IL-12} using SPIONs-PAA-PEI.

2. Materials and methods

2.1. De novo synthesis of SPIONs-PAA-PEI

SPIONs were synthesized by alkaline co-precipitation of ferrous and ferric sulfates, ($FeSO_4 \times 7H_2O$, 98% and ($Fe_2(SO_4)_3 \times xH_2O$)) (Alfa Aesar, Ward Hill, MA), in an aqueous solution according to the Massart method [24]. Briefly, 250 ml of 0.5 M aqueous solution containing ferric and ferrous ions in a weight-to-weight (w/w) ratio of 1.5:1 were precipitated with 150 ml of 25% ammonium hydroxide solution (NH_4OH) (Sigma-Aldrich, St. Louis, MO) under magnetic stirring at 600 rpm for 30 min at room temperature. After SPIONs were obtained, alkaline medium was removed and replaced with distilled water subsequent to magnetic decantation of SPIONs (repeated 3 times) in order to obtain a magnetic liquid, *i.e.* ferrofluid (FF). SPIONs were coated *in situ* with 45% (w/w) water solution of poly(acrilyc acid, sodium salt) (PAA) with molecular weight of 8 kDa (Sigma-Aldrich) by mixing 100 ml of FF-SPIONs and 100 ml of PAA water solution of equal mass concentrations at 10 mg/ml under magnetic stirring at 400 rpm for 5 min at room temperature. Thereafter FF-SPIONs-PAA was sterilized by filtration using 0.22 μm pore size syringe filter (Techno Plastic Products – TPP, Trasadingen, Switzerland). For the evaluation of physicochemical properties and for the experiments stock solution of the FF-SPIONs-PAA was diluted with distilled water to a working concentration of 1 mg/ml. Functionalization of SPIONs-PAA was performed directly prior to the experiments with branched cationic polymer polyethylenimine (PEI) with molecular weight of 25 kDa (Sigma-Aldrich). For *in vitro* experiments, FF-SPIONs-PAA at 1 mg/ml was added into 0.1 mg/ml PEI water solution at mass ratios 0.5:1, 0.6:1, 0.7:1, 0.8:1 and 0.9:1. For *in vivo* experiments, FF-SPIONs-PAA at 1 mg/ml was added into 1 mg/ml PEI water solution at the mass ratio 0.6:1.

2.1.1. Binding plasmid DNA to SPIONs-PAA-PEI

Two plasmid DNA (pDNA) were used for binding to SPIONs-PAA-PEI: pDNA containing reporter gene encoding GFP (pDNA^{GFP}) under the control of the constitutive cytomegalovirus (CMV) promoter (pCMV-EGFP-N1; Clontech, Mountain View, CA) or pDNA containing therapeutic gene encoding murine IL-12 (pDNA^{IL-12}) under the control of hybrid promoter EF-1α/HTLV, consisting of elongation factor 1α and 5′ untranslated region of the human T-cell leukemia virus, with open reading frame (ORF) (pORF-mIL-12; InvivoGen, San Diego, CA). Amplification of pDNA^{GFP} and pDNA^{IL-12} was performed in competent *Escherichia coli* cells (TOP10; Life Technologies, Carlsbad, CA), isolation using Qiagen Maxi-Endo-Free Kit (Qiagen, Hilden, Germany) and subjection to quality control and quantity determination using agarose gel electrophoresis and spectrophotometer (NanoDrop 2000; Thermo Scientific, Wilmington, DE). Dilution of pDNA^{GFP} and pDNA^{IL-12}, exhibiting the ratio between the absorbance at 260 nm and 280 nm wavelengths (A_{260}/A_{280}) more than 1.8, was made with endotoxin-free water to a working concentration of 1 mg/ml. SPIONs-PAA, PEI and pDNA^{GFP} or pDNA^{IL-12} were prepared at the mass ratio 0.6:1:1 (SPIONs-PAA-PEI-pDNA^{GFP} or SPIONs-PAA-PEI-pDNA^{IL-12}). The ability of SPIONs-PAA-PEI complexes to bind both pDNA was determined by 45 min electrophoresis at 100 V on a 1% (w/v) agarose gel stained with 0.5 μg/ml ethidium bromide. Visualization of the bands was performed under ultraviolet transilluminiscence (GelDoc-It TS 310; Ultra-Violet Products (UVP), Upland, CA). DNA ladder MassRuler™ DNA Ladders, ready-to-use (Thermo Fisher Scientific, Waltham, MA) was utilized.

2.1.2. Physicochemical properties of SPIONs, SPIONs-PAA, SPIONs-PAA-PEI and SPIONs-PAA-PEI-pDNA^{GFP}

Chemical composition and crystallographic structure of SPIONs and SPIONs-PAA were determined by X-ray diffractometry (XRD) measuring within the range of a diffraction angle 2Θ from 25° to 80° (AXS, D5005; Bruker, Billerica, MA). The mean crystallite size was calculated according to the broadening of the (311) characteristic peak of the XRD pattern using the Scherrer equation [25]. Size and shape of SPIONs and SPIONs-PAA were evaluated by transmission electron microscopy (TEM) (2000 FX with EDS AN10000; JEOL, Tokyo, Japan). The estimated size from TEM was obtained by measuring diameters of ten SPIONs and SPIONs-PAA from representative samples. Also, morphology of SPIONs-PAA-PEI and SPIONs-PAA-PEI-pDNA^{GFP} was visualized by TEM.

Magnetic characterization of SPIONs and SPIONs-PAA was conducted using a magnetometer (Quantum Design MPMS XL-5 SQUID, San Diego, CA) equipped with a 50 kOe magnet, operating in the temperature range 2–400 K. In the first set of measurements, the magnetization vs. the magnetic field curves, *M(H)*, and the magnetic susceptibility, $\chi(T)$, of dry SPIONs and SPIONs-PAA were determined at $T = 300$ K. In the second set of measurements, the magnetization vs. the magnetic field curves, *M(H)*, and the magnetic susceptibility, $\chi(T)$, of FF-SPIONs and FF-SPIONs-PAA were determined at $T = 300$ K.

The zeta (ζ) potentials of FF-SPIONs at pH = 9.5, FF-SPIONs-PAA at pH = 8.5 and FF-SPIONs-PAA-PEI at pH = 8 were determined by zetameter measuring electrophoretic mobility at 21 °C applied to the Henry equation (Zetasizer Nano ZS; Malvern Instruments, Malvern, UK).

2.2. Cell lines

Experiments were performed in two malignant melanoma cell lines, mouse B16F1 (LGC Standards, Teddington, UK) and human SK-MEL-28 (American Type Culture Collection (ATCC), Manassas, VA), and two normal cell lines, human mesothelial MeT-5A (ATCC) and mouse fibroblasts L929 (LGC Standards). B16F1, SK-MEL-28 and L929 cells were maintained in advanced minimum essential medium (MEM) (Life Technologies) whereas MeT-5A cells were maintained in advanced Roswell Park Memorial Institute (RPMI) 1640 medium (Life Technologies). Both media were supplemented with 5% fetal bovine serum (FBS; Life Technologies), 10 ml/l L-glutamine (Life Technologies), 100 U/ml penicillin (Grünenthal, Aachen, DE) and 50 μg/ml gentamicin (Krka, Novo mesto, Slovenia). Cells were grown in Petri dishes of 15 cm diameter (TPP) and incubated in a humidified atmosphere of 5% CO_2 at 37 °C until they reached at least 90% confluence. Then the medium was removed, cells were washed with phosphate-buffered saline (PBS) and detached with 0.25% trypsin/EDTA in Hank's buffer (Life Technologies). An equal volume of medium with FBS for trypsin inactivation was then added, cells were collected, centrifuged, counted and used for subsequent experiments.

2.2.1. Cytotoxicity of SPIONs-PAA-PEI-pDNA^{GFP}

Cytotoxicity of SPIONs-PAA-PEI bound to pDNA^{GFP} (SPIONs-PAA-PEI-pDNA^{GFP}) was tested on cells derived from B16F1, SK-MEL-28, L929 and MeT-5A cell lines by cell viability alamarBlue® (Life Technologies) assay measuring metabolic activity of cells. For the experiments 2.5×10^4 B16F1, 5×10^4 SK-MEL-28, 2.5×10^4 L929 and 7.5×10^4 MeT-5A cells were plated in 1 ml of cell culture medium on clear-bottomed 24-well plates (TPP). Immediately thereafter SPIONs-PAA, PEI and pDNA^{GFP} alone were added to cells in concentrations of 1.2 μg/ml, 2 μg/ml and 2 μg/ml, respectively. SPIONs-PAA-PEI complexes, PEI-pDNA^{GFP} and SPIONs-PAA-PEI-pDNA^{GFP} transfection complexes were prepared at mass ratios 0.6:1, 1:1 and 0.6:1:1, respectively, and added to cells at same concentrations as described above. Cells were either directly incubated or exposed to Nd-Fe-B magnets with surface magnetic flux density $B = 403$ mT and magnetic gradient $G = 38$ T/m (*i.e.* an external magnetic field) for 15 min. After 72 h incubation, 500 μl of cell culture medium was removed and 50 μl of alamarBlue® reagent (Life Technologies) was added, followed by 2-h incubation. The fluorescence of formed resorufin product was quantified using a fluorescence microplate reader (Infinite F200, Tecan, Männedorf, Switzerland) at 560 nm excitation wavelength and 590 nm emission wavelength. Cell survivals of exposed cells are presented as the percentages of the fluorescence obtained from untreated control cells.

2.2.2. Internalization of SPIONs-PAA-PEI-pDNA^{GFP} into cells

Internalization of SPIONs-PAA-PEI bound to pDNA^{GFP} (SPIONs-PAA-PEI-pDNA^{GFP}) into cells was evaluated qualitatively by TEM (CM100; Philips, Amsterdam, the Netherlands) and quantitatively by inductively coupled plasma mass spectrometer (ICP-MS) (Agilent 7700, Tokyo, Japan) determining iron (Fe) concentrations in

the samples of digested cells at m/z 56 and 57. Internalization of SPIONs-PAA-PEI-pDNA^{GFP} corresponds to the concentration of Fe in the samples, which is presented as the amount of Fe per cell normalized to control cells. For the experiments 5×10^4 B16F1, 1×10^5 SK-MEL-28, 5×10^4 L929 and 1.5×10^5 MeT-5A cells were plated in 1 ml of cell culture medium on clear-bottomed, 24-well plates (TPP). After 24 h or 48 h of incubation, complexes of SPIONs-PAA, PEI and pDNA^{GFP} were prepared at the mass ratio of 0.6:1:1, respectively, and given to cells at pDNA^{GFP} concentration of 2 μg/ml. Cells were exposed to an external magnetic field for 15 min. After 4 h or 24 h of incubation, the medium was removed and cells were washed with PBS for qualitative and quantitative determination of internalization. To determine the internalization of SPIONs-PAA-PEI-pDNA^{GFP} qualitatively, cells were fixed in a mixture of 4% (w/v) paraformaldehyde and 2.5% (v/v) glutaraldehyde in 0.1 M cacodylate buffer, pH 7.4, for 1 h at 4 °C. Post-fixation was carried out in 1% osmium tetroxide in 0.1 M cacodylate buffer for 2 h, followed by dehydration in graded ethanol and embedding in Epon 812 resin. Ultrathin sections (60 nm) were cut, counterstained with uranyl acetate and lead citrate and examined with TEM. To determine the internalization of SPIONs-PAA-PEI-pDNA^{GFP} quantitatively, cells were trypsinized, counted, collected in 4.5 ml cryo tubes (BD Biosciences, Two Oak Park, Bedford, MA) and stored at −18 °C. Prior to analysis, samples were equilibrated to room temperature and digested with a mixture of 0.2 ml 65% nitric acid and 0.2 ml 30% hydrogen peroxide by incubation at 90 °C for at least 24 h to obtain clear solutions. Samples were then diluted with water to 10 mL for the analysis with ICP-MS.

2.2.3. Magnetofection of cells with pDNA^{GFP} using SPIONs-PAA-PEI

To optimize the mass ratio between SPIONs-PAA, PEI and pDNA^{GFP} for magnetofection of cells using SPIONs-PAA-PEI, 5×10^4 B16F1, 1×10^5 SK-MEL-28, 5×10^4 L929 and 1.5×10^5 MeT-5A cells were plated in 1 ml of cell culture medium on clear-bottomed, 24-well plates. After 24 h of incubation, transfection complexes of SPIONs-PAA, PEI and pDNA^{GFP} were prepared at mass ratios from 0.5:1:1 to 0.9:1:1 and added to cells at pDNA^{GFP} concentration of 2 μg/ml. Cells were exposed to an external magnetic field for 15 min. After 24-h incubation, transfection efficacy was evaluated qualitatively with fluorescent microscope by recording images with digital camera (Olympus DP50) attached to fluorescent microscope (Olympus IX70, Hamburg, Germany) at 488 nm excitation wavelength and 507 nm emission wavelength. The differences in transfection of cells with pDNA^{GFP} between the absence and presence of an external magnetic field are presented as potentiating factors. Thereafter cells were trypsinized, collected in 15 ml conical falcon tubes (TPP) and centrifuged. The supernatant was removed and cells were resuspended to 5 ml polystyrene round-bottom tubes (BD Biosciences) in 1 ml of PBS for quantitative determination of transfection efficacy with flow cytometer (BD FACSCanto II; Becton Dickinson, San Jose, CA), identifying the percentage of GFP-positive (fluorescent) cells and measuring the median fluorescence intensity of the GFP. Statistics between the magnetofection efficacies using SPIONs-PAA-PEI, prepared as SPIONs-PAA-PEI-pDNA^{GFP}, at different mass ratios were analyzed by one way ANOVA. Statistics between the transfection efficacies using SPIONs-PAA-PEI in the absence and presence of an external magnetic field at the particular mass ratio were analyzed by Student's t-test.

Furthermore, comparison of the transfection efficacy of B16F1 cells with pDNA^{GFP} was made between: SPIONs-PAA-PEI prepared as SPIONs-PAA-PEI-pDNA^{GFP} at the mass ratio 0.6:1:1, PEI prepared as PEI-pDNA^{GFP} at the mass ratio 1:1, 3 different commercially available magnetic nanoparticles for magnetofection (CombiMAG and PolyMag purchased at chemicell GmbH, Berlin, Germany and MATra bought from IBA GmbH, Göttingen, Germany), electroporation, lipofection using Lipofectamine™ 2000 (Life Technologies) and SPIONs-PAA-PEI in the absence of an external magnetic field. Cells for transfection with PEI and SPIONs-PAA-PEI in the absence and presence of an external magnetic field as well as for electroporation were maintained in the medium as described above whereas cells for magnetofection with commercially available magnetic nanoparticles and lipofection were maintained in MEM, supplemented with 10% FBS and 10 ml/l L-glutamin. For transfection with PEI and SPIONs-PAA-PEI in the absence and presence of an external magnetic field, 5×10^4 cells were plated in 1 ml of cell culture medium on clear-bottomed, 24-well plates (TPP). After 24-h incubation, 2 μg/ml of pDNA^{GFP} was prepared as PEI-pDNA^{GFP} and SPIONs-PAA-PEI-pDNA^{GFP} at mass ratio of 1:1 and 0.6:1:1, respectively, and added to cells. Cells transfected with SPIONs-PAA-PEI-pDNA^{GFP} were either exposed to Nd-Fe-B magnets for 15 min or not. After 24 h of incubation, cells were prepared for analysis by flow cytometer as described above. For electroporation a dense cell suspension with a concentration of 1×10^6 cells and 10 μg of pDNA^{GFP} in 50 μl of electroporation buffer [26] was placed between two flat parallel stainless steel electrodes with a 2 mm gap connected to the GT-1 electroporator (University of Ljubljana, Faculty of Electrical Engineering, Ljubljana, Slovenia) and subjected to 8 square-wave electric pulses with an amplitude per distance ratio 600 V/cm, 5 ms duration time, and 1 Hz repetition frequency. After electroporation, cells were incubated for 5 min at the room temperature and then plated to 6 cm diameter Petri dishes (TPP). After 24-h incubation, cells were prepared for analysis by flow cytometer as described above. For lipofection and magnetofection with commercially available magnetic nanoparticles either 2.5×10^4 or 5×10^4 cells were plated in 1 ml of cell culture medium on clear-bottomed, 24-well plates (TPP). After 24-h incubation, 1.7 μg/ml of pDNA^{GFP} was used for lipofection in accordance to manufacturer's instructions whereas for magnetofection with commercially available magnetic nanoparticles 4 μg/ml of pDNA^{GFP} was coupled to nanoparticles according to the instructions of the manufacturer and given to cells with subsequent 15-min exposure to Nd-Fe-B magnets. After 24-h incubation, cells were prepared for analysis by flow cytometer as described above.

2.2.4. Magnetofection of cells with pDNA^{IL-12} using SPIONs-PAA-PEI

The comparison of the transfection efficacy of B16F1 cells with pDNA^{IL-12} was made between: magnetofection using SPIONs-PAA-PEI prepared as SPIONs-PAA-PEI-pDNA^{IL-12} at the mass ratio 0.6:1:1, PEI prepared as PEI-pDNA^{IL-12} at the mass ratio 1:1, electroporation, lipofection and SPIONs-PAA-PEI in the absence of magnetic field. The transfections of cells with pDNA^{IL-12} was performed likewise the transfection of pDNA^{GFP}-based experiments. After either 24-h incubation, the medium was transferred into 1.5 ml cryo tubes (Corning Incorporated, Corning, NY) and centrifuged in order to eliminate cell debris. Thereafter the supernatant was analyzed for the amount of IL-12 p70 by enzyme-linked immunosorbent assay (ELISA) kits (R&D Systems, Minneapolis, MN) in accordance to the manufacturer's instructions. Transfection efficacy is presented in picograms of secreted biologically active heterodimer p70 of IL-12 per cell.

2.3. Mice

In vivo experiments were performed on female BALB/c and C57Bl/6 mice obtained from the Institute of Pathology, Faculty of Medicine, University of Ljubljana, Slovenia. At the beginning of the experiments mice were 10–12 weeks old and were housed in specific pathogen free colony at constant room temperature 20–24 °C, relative humidity 55 ± 10% and 12 h light/dark cycle. Food and water were provided *ad libitum* unless otherwise stated. Animals were subjected to an adaptation period of 7–10 days before the experiments were carried out. All procedures were performed in compliance with the official guidelines of the Ministry of Agriculture, Forestry and Food of the Republic of Slovenia (permission no. 34401-11/2009/6).

2.3.1. In vivo acute toxicity and biodistribution of SPIONs-PAA and SPIONs-PAA-PEI-pDNA^{GFP}

Acute toxicity and biodistribution of SPIONs-PAA and SPIONs-PAA-PEI bound to pDNA^{GFP} (SPIONs-PAA-PEI-pDNA^{GFP}) were assessed in BALB/c mice. Acute toxicity of SPIONs-PAA was evaluated using Up-and-Down Procedure (UDP) protocol by the Organization for Economic Co-operation and Development (OECD). Biodistribution of SPIONs-PAA and SPIONs-PAA-PEI-pDNA^{GFP} was determined quantitatively by measuring iron concentration in samples of digested internal organs, *i.e.* lungs, heart, spleen, liver and kidneys, using ICP-MS, and qualitatively by recording images of histological specimens of liver with digital camera (Nikon DXM1200F; Nikon, Tokyo, Japan) attached to light microscope (Nikon Eclipse 80i). According to the OECD guidelines, food was restrained 3 h before and 1 h after the experiment whereas water was provided *ad libitum*. For the acute toxicity determination assessing the median lethal dose (LD_{50}) mice were injected intraperitoneally (i.p.) with 1 ml of high doses of SPIONs-PAA (175 mg/kg and 550 mg/kg). The highest dose suggested by the guidelines (2000 mg/kg) was not possible to inject due to the restricted i.p. injection volume and limited highest concentration of SPIONs-PAA stock solution. Additionally, body weight was monitored by weighing mice at the commencement and throughout the experiment every 4 days after the initial administration of SPIONs-PAA. Changes in body weight are presented as the ratios of the intermediate and final body weights to the initial body weight. Based on the results of our *in vitro* experiments and regarding pDNA^{IL-12} dosage optimization after i.t. administration followed by electroporation of tumors [27], three mice per group were also injected i.p. with low doses of SPIONs-PAA (1.2 mg/kg) and SPIONs-PAA-PEI-pDNA^{GFP} (1.2-2-2 mg/kg, respectively). Control group of animals was injected i.p. with distilled water in the same volume as SPIONs-PAA and SPIONs-PAA-PEI-pDNA^{GFP} were given (1 ml). Animals were sacrificed 14 days after the commencement of the experiment. Organs were removed, weighted and stored in 4 ml cryo vials (BD Biosciences) at −18 °C for ICP-MS analysis. Before analysis, microwave digestion of organs was applied, and then the measurement was performed likewise the quantitative internalization of SPIONs-PAA and SPIONs-PAA-PEI-pDNA^{GFP} into cells. Additionally, qualitative evaluation of biodistribution of SPIONs-PAA was made in liver, which was immediately after the excision fixed in 10% (w/v) buffered formalin phosphate and embedded in paraffin. From paraffin 10 μm thick sections were cut and stained with Perl's Prussian blue histochemical method. The Perls histochemical reaction is adequate for the detection of iron as ferritin and hemosiderin in higher vertebrates [28].

2.3.2. Magnetofection of tumors with pDNA^{GFP} using SPIONs-PAA-PEI

Magnetofection of B16F1 melanoma tumors, syngeneic to C57Bl/6 mice, and TS/A mammary adenocarcinoma tumors, syngeneic to BALB/c mice, with pDNA^{GFP} was evaluated in frozen tumor sections, which were examined for the GFP level and spatial distribution by recording images with digital camera (Olympus DP72) attached to fluorescent microscope (Olympus BX51). Tumors were induced by inoculating 1.0×10^6 B16F1 cells or 2.0×10^6 TS/A cells in 0.1 ml of 0.9% NaCl subcutaneously into the right flanks of mice. Cells of both cell lines were prepared from *in vitro* cultures growing in advanced MEM. After 7–9 days, when the tumors reached approx. 40 mm^3, mice were randomly divided into 6 groups consisting of 3

animals and subjected to different experimental protocols for 3 days consecutively. First group of animals was injected intratumorally (i.t.) with 40 μl of distilled water. Second group of animals was injected i.t. 15 μg of pDNA^{GFP} in 40 μl of endotoxin-free water. Third group of animals was injected i.t. with 15 μg of pDNA^{GFP} prepared in 40 μl of PEI-pDNA^{GFP} complexes at the mass ratio 1:1. Fourth and fifth group of animals were injected i.t. with 15 μg of pDNA^{GFP} prepared in 40 μl of SPIONs-PAA-PEI-pDNA^{GFP} complexes at the mass ratio of 0.6:1:1. Thereafter, Nd-Fe-B magnets (same magnets as used for *in vitro* experiments) were placed above the tumors of the fourth group and fixed with the tape for 30 min. Sixth group of animals was injected i.t. with 15 μg of pDNA^{GFP} in 40 μl of endotoxin-free water. After 10 min, electroporation of tumors was performed by applying eight square-wave electric pulses, delivered in 2 sets of 4 pulses in perpendicular directions, at a frequency of 1 Hz, amplitude over distance ratio of 600 V/cm and 5 ms duration through 2 parallel stainless steel electrodes with a 7 mm gap connected to GT-1 electroporator. All injections were performed using 0.3 ml insulin syringes with 28-gaugee needles (Terumo, Tokyo, Japan) on anesthetized animals. Also, fourth group of animals was subjected to anesthesia during the fixation of Nd-Fe-B magnets above the tumors. General anesthesia was induced and maintained by placing mice in a clear plastic chamber while administering 1.5–3% vapor set of isoflurane with oxygen flow at 1 l/min (Draeger, Lübeck, Germany). Tumors were excised 24 h after the last injection, embedded in Tissue-Tek OCT Compound (Sakura Finetek, Torrance, CA) and stored at −18 °C. Frozen tumor sections of 20 μm were cut every 150 μm of the tumor with cryostat (Leica CM1850; Leica Mycrosystems, Wetzlar, Germany) for the GFP level and spatial distribution examination.

2.3.3. Magnetofection of tumors with pDNA^{IL-12} using SPIONs-PAA-PEI

For the proof-of-principle, transfection of TS/A tumors with pDNA^{IL-12} was performed in BALB/c mice. Transfection efficacy of tumors was determined by calculating tumor volumes after measuring 3 orthogonal tumor diameters (e_1, e_2 and e_3) with Vernier caliper, using the formula $V = \frac{\pi \times e_1 \times e_2 \times e_3}{6}$. TS/A tumors were induced likewise the tumors for the pDNA^{GFP}-based experiments. After 7–9 days, when the tumors reached approx. 40 mm^3, mice were randomly divided into 9 groups consisting of 4 or 5 animals and subjected to different experimental protocols for 3 days consecutively. The protocol for the first six groups was the same as for the pDNA^{GFP}-based experiments. Seventh group of animals was subjected only to electric pulses, which were delivered in the same way as for the pDNA^{GFP}-based experiments. Eighth group of animals was injected i.t. 15 μg of PEI in 40 μl of endotoxin-free water. Ninth group of animals was injected i.t. 9 μg of SPIONs-PAA in 40 μl of endotoxin-free water with subsequent exposure to Nd-Fe-B magnets for 30 min that were placed above the tumors with the tape. Tumor growth and regression was monitored until the tumors reached between 300 and 350 mm^3; then the animals were euthanized. Tumor growth delay was calculated when the mean value of the tumor volume of all experimental groups reached 200 mm^3 because the tumors of SPIONs-PAA-PEI-pDNA^{IL-12}-treated mice and after pDNA^{IL-12} electrotransfer started to delay in growth after they had already reached doubling or tripling volume.

2.4. Statistical analysis

All quantitative data were tested for normality of distribution by Shapiro-Wilk test and are presented as means ± standard errors (s.e.m.). Student's *t*-test was used to evaluate the differences in the transfection efficacy between the absence and presence of magnetic field regarding optimization of magnetofection of cells with pDNA^{GFP} using SPIONs-PAA-PEI. All other quantitative data were analyzed by one way ANOVA, and tested for significance by Holm-Sidak test. Alpha level was set to 0.05. When *P* values were 0.05 or less, differences were considered statistically significant. All statistical analyses were performed by SigmaPlot 11 (Systat Software, San Jose, CA).

3. Results

3.1. De novo synthesis of SPIONs-PAA-PEI

We synthesized SPIONs for magnetofection by alkaline co-precipitation of ferrous and ferric ions in aqueous solution according to the Massart method [24]. To increase magnetofection efficacy and reduce PEI-related cytotoxicity, we coated SPIONs *in situ* with pH-responsive anionic polymer PAA and functionalized obtained SPIONs-PAA with cationic polymer PEI through electrostatic interaction between highly negative surface of SPIONs-PAA and positively charged polycation PEI. Functionalization of SPIONs-PAA with PEI was performed directly prior to the pDNAs binding due to incipient stability of the ferrofluid containing SPIONs-PAA-PEI. All results regarding physicochemical properties of SPIONs, SPIONs-PAA and SPIONs-PAA-PEI stand for a representative sample.

3.1.1. Physicochemical properties of SPIONs, SPIONs-PAA, SPIONs-PAA-PEI and SPIONs-PAA-PEI-pDNA^{GFP}

From the TEM images (Fig. 1a), diameter of spherical SPIONs was estimated to be 8 ± 1 nm whereas estimated diameter of SPIONs-PAA was 10 ± 1 nm. After functionalization of SPIONs-PAA with PEI (SPIONs-PAA-PEI), less than 2 nm-thick amorphous edge around the crystalline SPIONs-PAA was observed. After binding pDNA^{GFP} to SPIONs-PAA-PEI, a bubble-like-formation around clusters of SPIONs-PAA-PEI was noted. Crystallographic structure of SPIONs and SPIONs-PAA was iron oxide maghemite (γ-Fe_2O_3) as observed from the XRD patterns (Fig. 1b). Immobilization of pDNA^{GFP} and pDNA^{IL-12} was observed after binding to SPIONs-PAA-PEI and PEI by agarose gel electrophoresis (Fig. 1c). Contrariwise, highly negative surface of SPIONs-PAA without PEI functionalization remained unattached to electronegative oxygens of phosphate groups of pDNA.

The ferrimagnetic shape of *M(H)* curves and saturated magnetization values of dry SPIONs and SPIONs-PAA (amounting $M_0 = 69$ emu/g and $M_0 = 62$ emu/g, respectively) were typical for γ-Fe_2O_3-composed nanoparticles (Fig. 1d). The zero-field-cooled (zfc) and field-cooled (fc) magnetic susceptibilities, $\chi = M/H$, of dry SPIONs and SPIONs-PAA, measured in a magnetic field $H = 100$ Oe, showed χ_{zfc} - χ_{fc} splitting at about 280 K, whereas a broad maximum in χ_{zfc} was observed at the temperature $T_B = 185$ K. This could be associated with the superparamagnetic blocking temperature below which SPIONs' spin reorientation is frozen on the experimental time scale. The $T_B = 185$ K value was consistent with TEM-estimated diameters of SPIONs and SPIONs-PAA, as for larger SPIONs T_B shifts above the room temperature. Similarly, χ_{zfc} - χ_{fc} splitting and $T_B \approx 300$ K were observed for SPIONs-PAA, where slightly higher values, as compared to SPIONs, very likely originated from their slightly larger size. Magnetic characterization of dry SPIONs and SPIONs-PAA thus confirmed their superparamagnetic nature and small size with diameters in the range 8–10 nm. The *M(H)* curves and the magnetic susceptibility $\chi = M/H$ of ferrofluids (FFs), denoting water-based suspension of SPIONs (FF-SPIONs) and SPIONs-PAA (FF-SPIONs-PAA), were also determined. The *M(H)* shapes remained those of the dry samples (the diamagnetic susceptibility of water is negligible as compared to the ferrimagnetic susceptibility of γ-Fe_2O_3-composed SPIONs). The difference in magnetization values between FF-SPIONs and FF-SPIONs-PAA originated from different concentration of nanoparticles in the suspensions (FF-SPIONs > FF-SPIONs-PAA). The temperature-dependent zfc and fc susceptibilities of FFs displayed discontinuities in the vicinity of $T = 0\ ^\circ C = 273$ K (marked by vertical dashed line), which was a consequence of FFs freezing upon cooling and melting upon heating. By measuring the fc susceptibility in a cooling run, starting at 300 K, FFs freezed at 260 K. In the zfc susceptibility measurements performed in a heating run, starting at 2 K, melting of FFs started at 273 K.

Zeta potentials of FF-SPIONs at pH 9.5 and FF-SPIONs-PAA at pH 8.5 were $\zeta = -24 \pm 2$ mV and $\zeta = -47 \pm 2$ mV, respectively, indicating negative surface charge of SPIONs as well as SPIONs-PAA and good stability of FF-SPIONs-PAA due to strong mutual electrostatic repulsion. Zeta potential of the FF-SPIONs-PAA-PEI at pH 8 was $\zeta = 20 \pm 1$ mV, indicating positive surface charge of SPIONs-PAA-PEI due to the functionalization of SPIONs-PAA's surface with PEI.

3.2. In vitro

3.2.1. Cytotoxicity of SPIONs-PAA-PEI and SPIONs-PAA-PEI-pDNA^{GFP} on cells of different cell lines

We tested cytotoxicity of SPIONs-PAA-PEI and SPIONs-PAA-PEI bound to pDNA^{GFP} (SPIONs-PAA-PEI-pDNA^{GFP}) on mouse melanoma B16F1 cells, human melanoma SK-MEL-28 cells, mouse fibroblasts L929 and human mesothelial MeT-5A cells, and

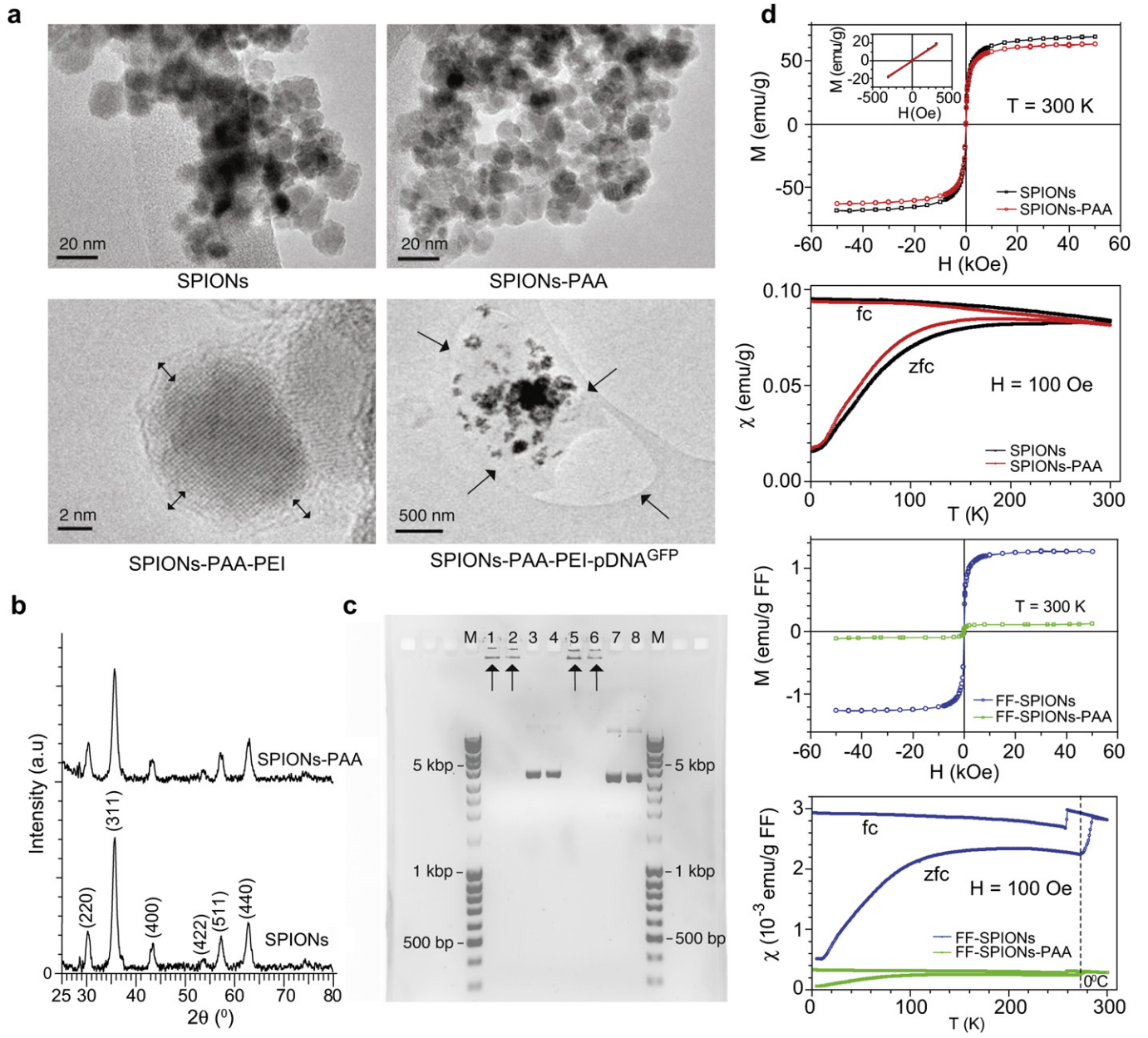

Fig. 1. Physicochemical properties of SPIONs, SPIONs-PAA, SPIONs-PAA-PEI and SPIONs-PAA-PEI-pDNA^{GFP}: (a) Transmission electron micrographs of spherical SPIONs, SPIONs-PAA, SPIONs-PAA-PEI and SPIONs-PAA-PEI-pDNA^{GFP}. 12 nm-sized SPION-PAA-PEI has an amorphous 1–2 nm edge (double arrows). SPIONs-PAA-PEI are entrapped inside organic bubble-like-formation (pDNA) forming SPIONs-PAA-PEI-pDNA^{GFP} (arrows). (b) X-ray diffractograms of SPIONs and SPIONs-PAA exhibit characteristic peaks for iron oxide maghemite (γ-Fe_2O_3). (c) Retardation of pDNA^{IL-12} and pDNA^{GFP} bound to SPIONs-PAA-PEI (lanes 1 and 5, respectively), and to PEI (lanes 2 and 6, respectively) (arrows). Separation of pDNA^{IL-12} and pDNA^{GFP} (lanes 3 and 7, respectively) as well as pDNA^{IL-12} and pDNA^{GFP} that did not bound to SPIONs-PAA (lanes 4 and 8, respectively). Molecular weight markers (M). (d) *M(H)* curves, the saturated magnetization and temperature dependent zero-field-cooled (zfc) and field-cooled (fc) magnetic susceptibilities, $\chi = M/H$, of dry SPIONs and SPIONs-PAA and ferrofluids containing SPIONs (FF-SPIONs) and SPIONs-PAA (FF-SPIONs-PAA). All data are for a representative sample.

compared it to cytotoxicity of PEI-pDNA^{GFP}. No additional cytotoxicity of an external magnetic field generated by Nd-Fe-B magnets on cells of all four cell lines in comparison to cells not exposed to an external magnetic field was observed (Fig. 2a). Therefore, results regarding cytotoxicity of a certain substance as well as comparisons between the substances will be interpreted referring to the presence of an external magnetic field. No substance decreased cell survival below 50% in all cell lines. In general, cells of all cell lines exhibited similar toxicity-related patterns to added substances. Only for MeT-5A cells, survival was significantly decreased after exposure to pDNA^{GFP} (60%) in comparison to SPIONs-PAA, PEI and SPIONs-PAA-PEI. Pronounced sensibility of MeT-5A cells to pDNA^{GFP} might be due to their spontaneous transfection which we observed during the experiments (data not shown). Survivals of cells of all cell lines, treated with SPIONs-PAA-PEI, alternated between 82% and 86%. Binding of pDNA^{GFP} to SPIONs-PAA-PEI (SPIONs-PAA-PEI-pDNA^{GFP}) significantly decreased cell survival, probably due to the compromised cell membrane integrity after internalization of SPIONs-PAA-PEI-pDNA^{GFP}, which was followed by magnetofection (See further results). Similar was observed after treatments of cells with PEI-pDNA^{GFP}. SPIONs-PAA-PEI-pDNA^{GFP} displayed tendency of being less cytotoxic than PEI-pDNA^{GFP} in all cell lines, however, only in L929 cells significant difference in cell survival after the exposure to

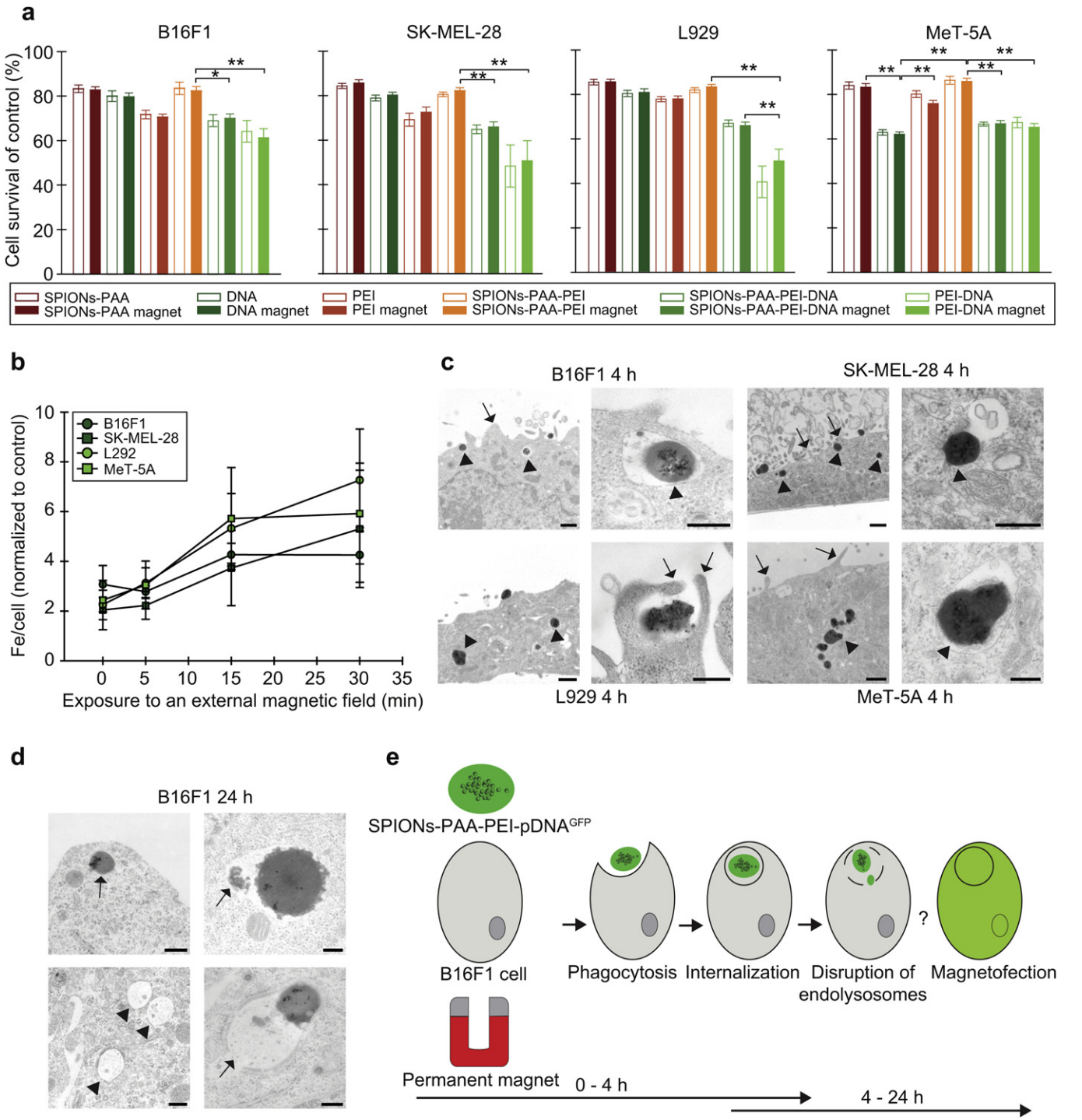

Fig. 2. Cytotoxicity and internalization of SPIONs-PAA-PEI-pDNA^{GFP}: (a) Cytotoxicity of SPIONs-PAA-PEI and SPIONs-PAA-PEI-pDNA^{GFP} on B16F1, SK-MEL-28, L929 and MeT-5A cells in comparison to PEI-pDNA^{GFP} in the absence and presence of an external magnetic field. $^{*}P < 0.05$, $^{**}P < 0.01$, between the compared groups ($n = 12$). (b,c) Internalization of SPIONs-PAA-PEI-pDNA^{GFP} into cells of different cell lines after 4-h incubation with SPIONs-PAA-PEI-pDNA^{GFP}. (b) Quantitative determination of internalized SPIONs-PAA-PEI-pDNA^{GFP} corresponds to the Fe concentration per cell. (c) Transmission electron micrographs of B16F1, SK-MEL-28, L929 and MeT-5A cells with internalized SPIONs-PAA-PEI-pDNA^{GFP} complexes after 15-min exposure to an external magnetic field. SPIONs-PAA-PEI-pDNA^{GFP} inside endocytotic compartments with intact membranes (arrowheads). Pseudopodia-like formations (arrows) coinciding with the invagination of the cell membrane. Scale bar, 500 nm first and third column; 200 nm second and fourth column. (d) Internalization of SPIONs-PAA-PEI-pDNA^{GFP} into B16F1 cells after 24-h incubation with SPIONs-PAA-PEI-pDNA^{GFP} subsequent to 15-min exposure to an external magnetic field. Transmission electron micrographs (clockwise): The internalized SPIONs-PAA-PEI-pDNA^{GFP} inside the endocytotic compartment (arrow) beneath the cell surface. SPIONs-PAA-PEI-pDNA^{GFP} in the endocytotic compartment with intact membrane, and organic compound separation (arrow). SPIONs-PAA-PEI-pDNA^{GFP} in the endocytotic compartment with disrupted membrane (arrow). Vacuoles without SPIONs-PAA-PEI-pDNA^{GFP} (arrowheads). Scale bar, 200 nm. (e) Schematic showing the process of internalization of SPIONs-PAA-PEI-pDNA^{GFP} followed by subsequent magnetofection of the cell after exposure to an external magnetic field in a 24 h time scale.

SPIONs-PAA-PEI-pDNA^{GFP} (67%) and PEI-pDNA^{GFP} (50%) in disfavor to the latest was observed.

3.2.2. Internalization of SPIONs-PAA-PEI-pDNAGFP into cells

Internalization of SPIONs-PAA-PEI bound to pDNA^{GFP} (SPIONs-PAA-PEI-pDNA^{GFP}) was evaluated quantitatively and qualitatively. Quantitative analysis demonstrated internalization of SPIONs-PAA-PEI-pDNA^{GFP} into cells of all cell lines at 4 h after the incubation with SPIONs-PAA-PEI-pDNA^{GFP} and exposure to an external magnetic field for different time intervals (Fig. 2b). Internalization of SPIONs-PAA-PEI-pDNA^{GFP} corresponds to the cellular iron (Fe) concentration. No statistically significant differences in Fe concentration between the cell lines were noticed. In all cell lines directly proportional tendency between the time interval exposure to an external magnetic field and Fe concentration was found. However, no statistically significant differences in Fe concentration between 0 and 30 min exposures to an external magnetic field were determined. Additionally, in B16F1 and L929 cells plateau level at 15-min exposure to an external magnetic field was observed. According to these results, intermediate time interval exposure (15 min) to an external magnetic field was chosen for the implementation into further experiments for magnetofection of cells with pDNA^{GFP} or pDNA^{IL-12}.

In agreement with the results of quantitative analysis, at 4 h after incubation with SPIONs-PAA-PEI-pDNA^{GFP} that included 15-min exposure of cells to an external magnetic field, internalization of complexes was observed in cells of all cell lines (Fig. 2c). Due to the size of the complexes (approx. 200–400 nm), the cellular uptake was determined to be phagocytosis. Moreover, distinctive pseudopodia-like formations were observed in cells of all cell lines. The complexes were observed in the endocytotic compartments with intact membranes. No SPIONs-PAA-PEI-pDNA^{GFP} complexes outside the endocytotic compartments neither in the cytoplasm nor in the nucleus were observed. At 24 h after incubation with SPIONs-PAA-PEI-pDNA^{GFP}, the complexes were observed in the endocytotic compartments of B16F1 cells with intact as well as disrupted membranes (Fig. 2d). No SPIONs-PAA-PEI-pDNA^{GFP} were observed in the cytoplasm, however, separation of organic compound (pDNA^{GFP}) from the complexes within the endocytotic compartments and vacuoles without SPIONs-PAA-PEI-pDNA^{GFP} were detected. Schematic showing the processes of internalization of SPIONs-PAA-PEI-pDNA^{GFP} followed by subsequent magnetofection after exposure of a cell to an external magnetic field in a 24 h time scale (Fig. 2e).

3.2.3. Magnetofection of cells with pDNA^{GFP} using SPIONs-PAA-PEI

Magnetofection with pDNA^{GFP} using SPIONs-PAA-PEI was performed in four cell lines: B16F1, SK-MEL-28, L929 and MeT-5A, and compared to the transfection using PEI only (Fig. 3a). Optimization of magnetofection was conducted by preparing SPIONs-PAA, PEI and pDNA^{GFP} at different mass ratios. Among the cell lines B16F1 cells exhibited the highest percentage of fluorescent cells (47%) at the mass ratio of 0.6:1:1, however, MeT-5A cells displayed the highest fluorescence intensity (11,943 a.u.) at the mass ratio 0.5:1:1. The lowest percentage of fluorescent cells (2%) as well as the lowest fluorescence intensity (520 a.u.) was observed in L929 cells. The percentage of fluorescent SK-MEL-28 cells (13%) was similar to that of MeT-5A cells (12%), however, their fluorescence intensity (4,169 a.u.) was only higher than that of L929. In all cell lines, exposure of cells to an external magnetic field contributed to the increase in the percentage of fluorescent cells only at the mass ratio 0.9:1:1, however the highest percentage of fluorescent B16F1 cells was observed at the mass ratio 0.6:1:1. Interestingly, an external magnetic field did not contribute to the increase in the percentage of fluorescent B16F1 cells only at that mass ratio. In comparison to the transfection with pDNA^{GFP} using PEI prepared as PEI-pDNA^{GFP} at the mass ratio 1:1, significant increase in the percentage of fluorescent B16F1 cells at the mass ratio 0.6:1:1 was observed. According to all these results, mass ratio 0.6:1:1 was chosen to be implemented in further experiments on B16F1 cells (Fig. 3b).

Photomicrographs taken under fluorescence epi-illumination support the quantitative results with the GFP expression observed in all cell lines in the absence and presence of an external magnetic field (Fig. 3c). The GFP levels observed from the photomicrographs indicated differences in transfection efficacy at the level of the cell line as well as some alterations in the absence and presence of an external magnetic field were noticed. In agreement with the results obtained from quantitative analysis, B16F1 cells showed the highest GFP level whereas L929 cells resulted in the lowest.

Magnetofection of B16F1 cells with pDNA^{GFP} using SPIONs-PAA-PEI was compared to transfection using PEI, 3 commercially available magnetic nanoparticles, electroporation, lipofection and SPIONs-PAA-PEI in the absence of an external magnetic field (Fig. 3d). Magnetofection using SPIONs-PAA-PEI resulted in excellent transfection efficacy, which was comparable to electroporation, lipofection and SPIONs-PAA-PEI in the absence of an external magnetic field. However, SPIONs-PAA-PEI outperformed PEI and all commercially available magnetic nanoparticles for magnetofection either in the percentage of fluorescent cells or in the fluorescence intensity.

3.2.4. Magnetofection of cells with pDNA^{IL-12} using SPIONs-PAA-PEI

Magnetofection of B16F1 cells with pDNA^{IL-12} using SPIONs-PAA-PEI was compared to transfection using PEI, electroporation, lipofection and SPIONs-PAA-PEI in the absence of an external magnetic field (Fig. 3e). The secretion of IL-12 from B16F1 cells into medium was observed after transfection with all the methods tested. Magnetofection resulted in 12.6-fold and 7.2-fold increase in transfection efficiency in comparison to PEI and lipofection, respectively. No statistically significant differences in transfection efficacy using SPIONs-PAA-PEI in the absence and presence of magnetic were observed, however, IL-12 secretion was increased for 1.2-fold in the presence over the absence of an external magnetic field.

3.3. In vivo

3.3.1. Acute toxicity and biodistribution of SPIONs-PAA and SPIONs-PAA-PEI

The acute toxicity was determined according to the OECD guidelines. The i.p. administration of the highest dose injected, 550 mg/kg of SPIONs-PAA, did not result in any death in the time period of 14 days after injection. Therefore, LD_{50} determination was not possible. The highest dose suggested to be used by OECD guidelines (2000 mg/kg) was not possible to inject due to the restricted i.p. injection volume and limited highest concentration of SPIONs-PAA in stock solution. A slight but non-significant decrease in body weight was observed on day 4 after the first administration of SPIONs-PAA as well as distilled water, but after day 4 the body weight started to rise (Fig. 4a).

After the i.p. administration of 175 mg/kg and 550 mg/kg of SPIONs-PAA, Fe concentrations were elevated in spleen and liver (Fig. 4b). In spleen, Fe concentrations were increased for 1.9-fold and 2.5-fold after administration of 175 mg/kg and 550 mg/kg of SPIONs-PAA, respectively, in comparison to the Fe concentration measured in the spleen of control mice. Similarly in liver, Fe concentrations were increased after administration of 175 mg/kg and 550 mg/kg of SPIONs-PAA for 1.5-fold and 3.4-fold, respectively, in comparison to the Fe concentration measured in the liver

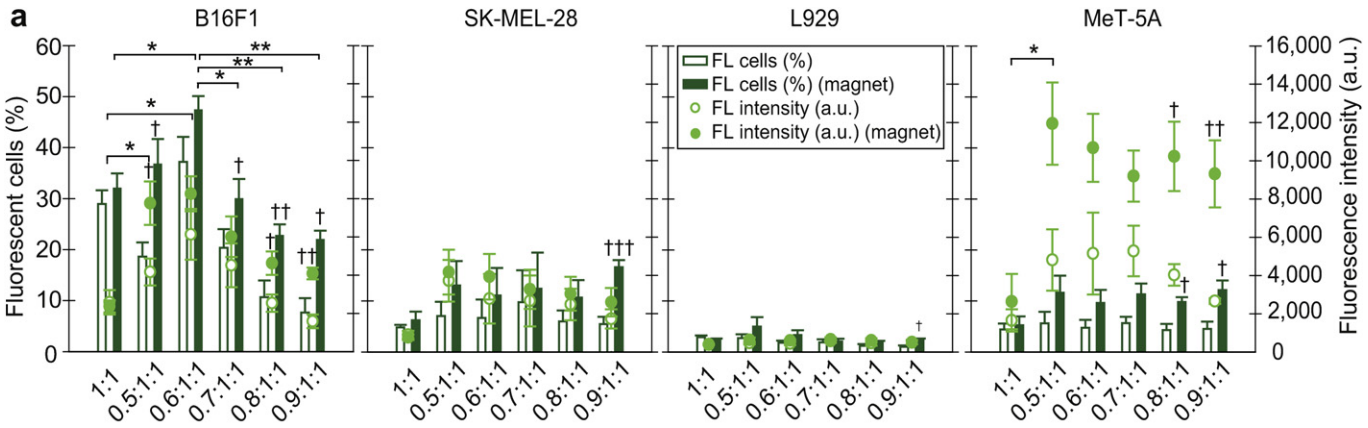

b

Cells	n	The GFP level after magnetofection (mean ± s.e.m.)	
		FL cells	FL intensity
B16F1	11	47.4 ± 2.7	8,254 ± 919
SK-MEL-28	4	11.1 ± 5.4	3,931 ± 1,196
L929	4	3.3 ± 0.9	607 ± 49
MeT-5A	4	9.6 ± 2.6	10,678 ± 1,779

Cells	n	Increase in the GFP level by exposure of cells to an external magnetic field (potentiating factor)	
		FL cells	FL intensity
B16F1	11	1.3	1.3
SK-MEL-28	4	1.7	1.4
L929	4	1.8	1.4
MeT-5A	4	2	2

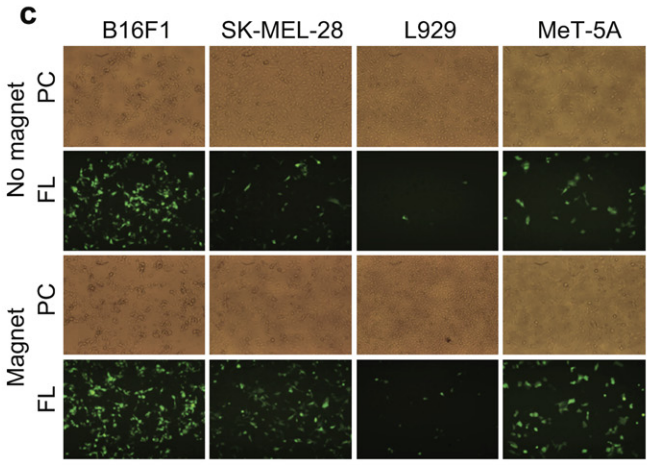

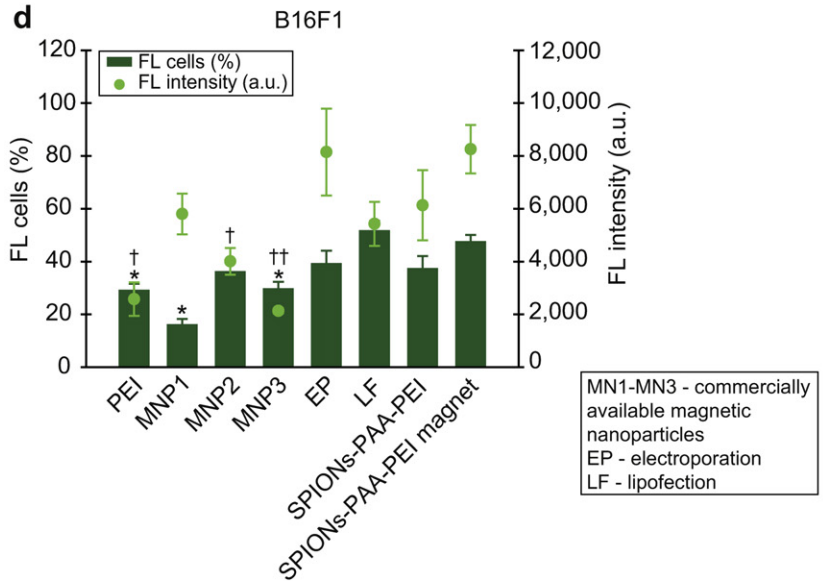

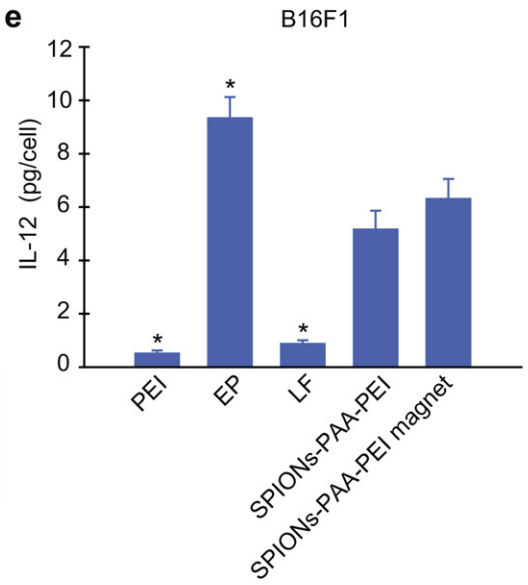

Fig. 3. Magnetofection of cells using SPIONs-PAA-PEI: (a) Determination of the GFP level, measured as the percentage of fluorescent (FL) cells and median fluorescence (FL) intensity, in B16F1, SK-MEL-28, L929 and MeT-5A cells after transfection with $pDNA^{GFP}$ using SPIONs-PAA-PEI prepared as SPIONs-PAA-PEI-$pDNA^{GFP}$ at mass ratios from 0.5:1:1 to 0.9:1:1 in the absence and presence of magnetic field. Mass ratio 1:1 denotes PEI-$pDNA^{GFP}$. $^{*}P < 0.01$, $^{**}P < 0.001$, comparison between mass ratios. $^{\dagger}P < 0.05$, $^{\dagger\dagger}P < 0.01$, $^{\dagger\dagger\dagger}P < 0.001$, compared to the absence of an external magnetic field ($n = 4$ or 11). (b) The GFP level and increase after magnetofection of cells using SPIONs-PAA-PEI prepared as SPIONs-PAA-PEI-$pDNA^{GFP}$ at the mass ratio 0.6:1:1. (c) Micrographs of B16F1, SK-MEL-28, L929 and MeT-5A cells after transfection with $pDNA^{GFP}$ using SPIONs-PAA-PEI prepared as SPIONs-PAA-PEI-$pDNA^{GFP}$ at the mass ratio 0.6:1:1 in the absence and presence of magnetic field under phase contrast (PC) and fluorescence epi-illumination (FL) (×60 magnification). (d,e) Magnetofection of B16F1 cells with $pDNA^{GFP}$ or $pDNA^{IL-12}$ using SPIONs-PAA-PEI, prepared as SPIONs-PAA-PEI-$pDNA^{GFP}$ or SPIONs-PAA-PEI-$pDNA^{IL-12}$ at the mass ratio 0.6:1:1, in comparison to other methods. (d) The GFP level in B16F1 cells. $^{*}P < 0.01$, compared to SPIONs-PAA-PEI magnet (FL cells). $^{\dagger}P < 0.05$, $^{\dagger\dagger}P < 0.01$, compared to SPIONs-PAA-PEI magnet (FL intensity) ($n = 7–13$). (e) The secretion of IL-12 from B16F1 cells.$^{*}P < 0.01$, compared to SPIONs-PAA-PEI magnet ($n = 3$).

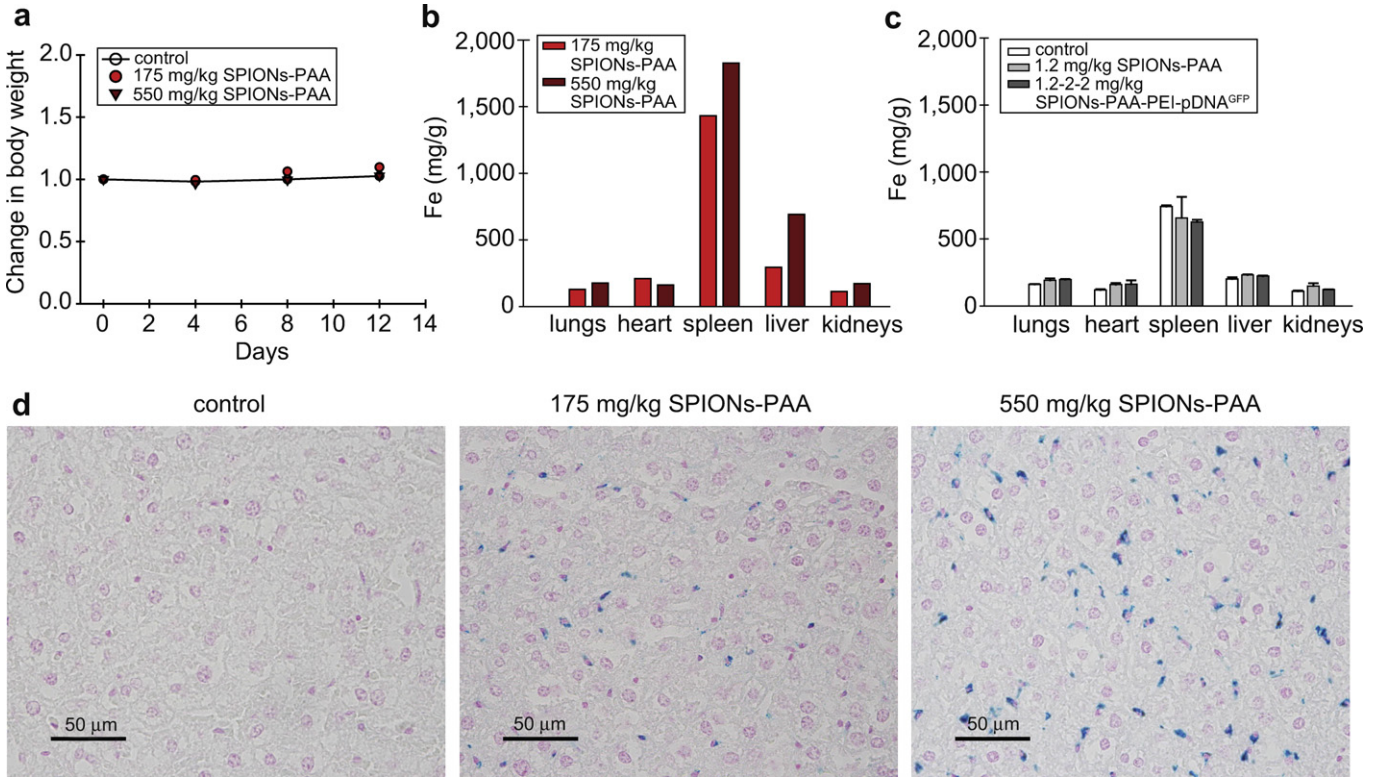

Fig. 4. Change in body weight after the i.p. administration of high doses of SPIONs-PAA and biodistribution of SPIONs-PAA and SPIONs-PAA-PEI-pDNA^{GFP} after i.p. administration of low and high doses: (a) Change in body weight. Symbols represent the ratios of intermediate and final body weights to initial body weight. The experiment was performed in one mouse per dosage due to the OECD guidelines. (b) Biodistribution of high doses of SPIONs-PAA. The experiment was performed in one mouse per dosage due to the OECD guidelines. Bars represent absolute values. (c) Biodistribution of low doses of SPIONs-PAA and SPIONs-PAA-PEI-pDNA^{GFP}. (d) Micrographs of mice liver stained with Perl's Prussian blue after administration of distilled water (control) and two different high doses of SPIONs-PAA.

of control mice. Based on the results of our *in vitro* experiments and regarding pDNA^{IL-12} dosage optimization after i.t. administration followed by electroporation of tumors [27], mice were also injected i.p. with low doses of SPIONs-PAA (1.2 mg/kg) and SPIONs-PAA-PEI-pDNA^{GFP} (1.2-2-2 mg/kg) to evaluate the biodistribution. No significant differences in Fe concentration within the organs between the control group and low doses-treated groups of mice with SPIONs-PAA and SPIONs-PAA-PEI-pDNA^{GFP} were detected (Fig. 4c).

In agreement with the results of quantitative analysis, Perl's Prussian blue staining of the control liver indicated SPIONs-PAA free organ whereas after the administration of high doses of SPIONs-PAA blue precipitates with Fe^{3+}, indicating the accumulation of SPIONs-PAA, in the phagocytes of the reticulo-endothelial system were detected (Fig. 4d).

3.3.2. *Magnetofection of tumors with pDNA^{GFP} using SPIONs-PAA-PEI*

Magnetofection of tumors with pDNA^{GFP} using SPIONs-PAA-PEI was tested in two tumor models: B16F1 melanoma syngeneic to C57Bl/6 mice due to the highest magnetofection efficacy of B16F1 cells *in vitro*, and TS/A mammary adenocarcinoma syngeneic to BALB/c mice, in which acute toxicity and biodistribution were determined. Also, we were interested in how weakly immunogenic TS/A mammary adenocarcinoma [29] would respond to immunogene therapy with pDNA^{IL-12}.

As demonstrated from the frozen tumor sections, magnetofection of B16F1 melanoma and TS/A mammary adenocarcinoma tumors with pDNA^{GFP} using SPIONs-PAA-PEI was effective (Fig. 5a). The GFP level in B16F1 tumors was observed either after 30-min exposure to an external magnetic field or in the absence of an external magnetic field. However, without an external magnetic field exposure, the GFP level in TS/A tumors after transfection with SPIONs-PAA-PEI was barely visible. Importantly, no transfection of both tumors with pDNA^{GFP} using PEI was observed (data not shown). Hence, by combining PEI with SPIONs-PAA, increased transfection efficiency *in vitro* was achieved and magnetofection of two different murine tumors was proved *in vivo*. Gene electrotransfer of tumors was used as a positive control since it is known and well established non-viral transfection method of tumors [30,31]. Gene electrotransfer resulted in homogenous GFP spatial distribution whereas after magnetofection scattered GFP spatial distribution was observed (Fig. 5a). The effect of an external magnetic field on magnetofection of melanoma B16F1 and mammary adenocarcinoma TS/A tumors with pDNA^{GFP} using SPIONs-PAA-PEI was more pronounced in TS/A than in B16F1 tumors.

3.3.3. *Magnetofection of tumors with pDNA^{IL-12} using SPIONs-PAA-PEI*

Magnetofection of TS/A mammary adenocarcinoma tumors with pDNA^{IL-12} using SPIONs-PAA-PEI resulted as effective treatment in BALB/c mice (Fig. 5b). Three consecutive treatments lead to statistically significant reduction in the tumor volume compared to non-treated tumors. The effect of the treatment was noticed 2 days after the completion of the treatment. The significant antitumor effect was seen only when the tumors were exposed to an external magnetic field whereas in the absence there was no antitumor effect. Gene electrotransfer of pDNA^{IL-12} has in other studies already resulted in tumor growth regression [27,32]. Thus, we used

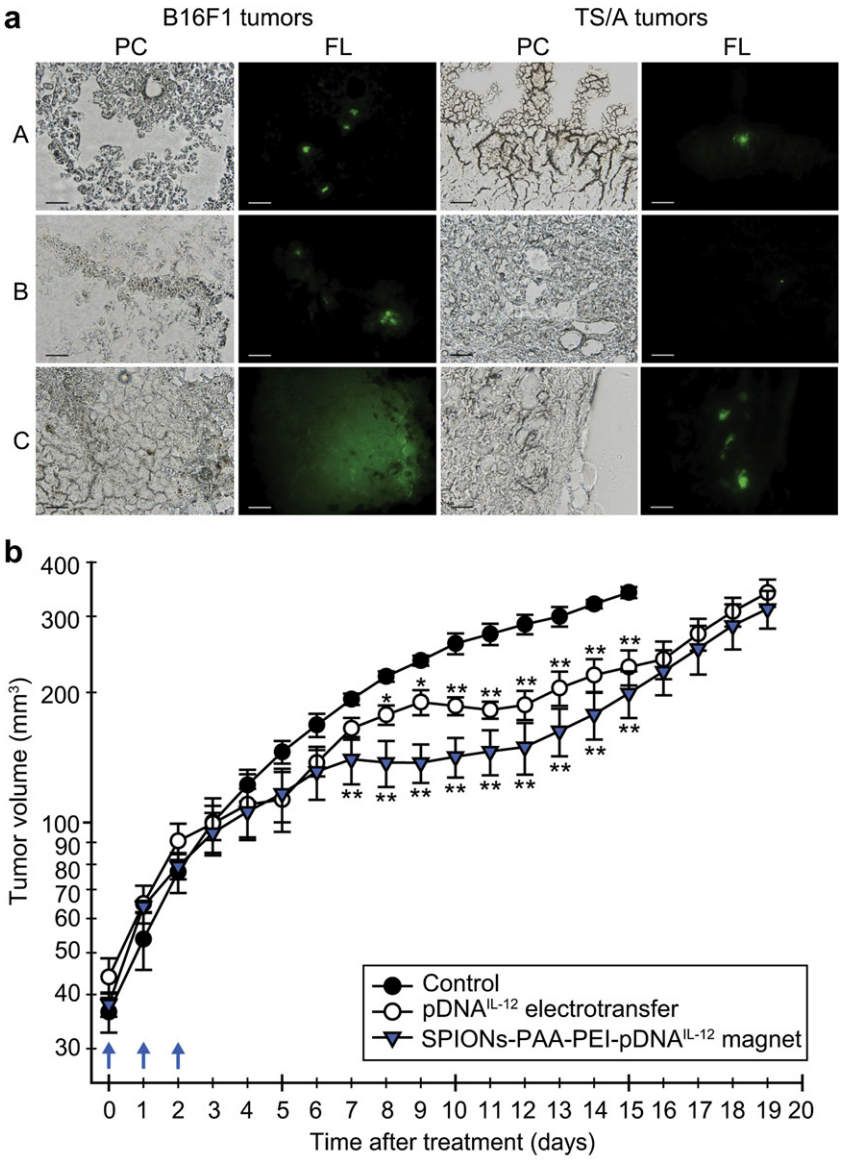

c

Experimental	*n*	*P*	Tumor growth delay (mean ± s.e.m.)
Control	5		0.0 ± 0.5
Distilled water, electric pulses	4	not significant	-1.3 ± 0.9
$pDNA^{IL-12}$	5	not significant	-0.3 ± 0.0
SPIONs-PAA magnet	5	not significant	0.8 ± 1.1
PEI-$pDNA^{IL-12}$	5	not significant	1.2 ± 1.3
PEI	4	not significant	2.2 ± 1.1
$pDNA^{IL-12}$ electrotransfer	5	< 0.01	6.6 ± 1.1
SPIONs-PAA-PEI-$pDNA^{IL-12}$	4	not significant	0.6 ± 0.5
SPIONs-PAA-PEI-$pDNA^{IL-12}$ magnet	5	< 0.01	7.8 ± 1.3

Fig. 5. Magnetofection of tumors with $pDNA^{GFP}$ or $pDNA^{IL-12}$ using SPIONs-PAA-PEI: (a) Micrographs of frozen murine melanoma B16F1 and mammary adenocarcinoma TS/A tumor sections under phase contrast (PC) and epi-fluorescence illumination (FL) after transfection with $pDNA^{GFP}$ using (A) magnetofection, (B) SPIONs-PAA-PEI in the absence of magnetic field, (C) electrotransfer. Scale bar, 50 μm. (b) Antitumor effect of i.t. administration of $pDNA^{IL-12}$ on TS/A mammary adenocarcinoma tumors after magnetofection with SPIONs-PAA-PEI and electrotransfer. Blue arrows represent three consecutive treatments with $pDNA^{IL-12}$. Tumor growth delay was calculated on the 10th day. (c) The effect of cancer immuno-gene therapy with $pDNA^{IL-12}$ on TS/A mammary adenocarcinoma tumors. $^{*}P < 0.05$, $^{**}P < 0.01$, compared to control ($n = 5$).

gene electrotransfer as a positive control, and similarly to magnetofection it resulted in statistically significant antitumor effect in comparison to untreated control tumors (Fig. 5c). Tumor growth delay was calculated at the tumor volume 200 mm^3 because tumors of SPIONs-PAA-PEI-pDNA^{IL-12}-treated mice and after pDNA^{IL-12} electrotransfer started to delay in growth after they had already reached doubling or tripling volume (Fig. 5b). The effect of magnetofection and gene electrotransfer was comparable: gene therapy of tumors with pDNA^{IL-12} resulted in 7.8 ± 1.3 and 6.6 ± 1.1 days tumor growth delays, respectively. In all the other control groups no antitumor effect was observed (Fig. 5c).

4. Discussion

Biocompatibility and biodistribution of every nanoparticulate delivery system should be determined since the physicochemical properties, such as size, shape and surface characteristics, might govern their brand new behavior and safety *in vitro* and *in vivo* [33]. *In vitro*, survival of cells of all cell lines was after treatment with SPIONs-PAA-PEI subsequent to 15-min exposure to an external magnetic field still around 80%, which is similar to the cytotoxicity of silica-coated SPIONs [34]. PEI-related cytotoxicity of PEI-pDNA^{GFP} reduced cell survival up to 50%, and was statistically significantly diminished by associating PEI-pDNA^{GFP} to SPIONs-PAA only in fibroblasts L929. In general, SPIONs-PAA-PEI-pDNA^{GFP} decreased survival of cells to approximately 70%, which indicated that they were not vastly cytotoxic, and could be further used in animal studies. *In vivo*, i.p. administration of 175 mg/kg and 550 mg/kg of SPIONs-PAA did not reach the LD_{50}. To date, there are no other reports about the *in vivo* toxicity of γ-Fe_2O_3-composed, PAA-coated and PEI-functionalized SPIONs. Different research groups selected different coatings, functionalization and cargos for SPIONs as delivery systems, thus the comparison between the studies evaluating LD_{50} of so diversified SPIONs is virtually impossible. Nonetheless, acute toxicity-based study in mice showed that LD_{50} for magnetite (Fe_3O_4)-composed and dextran-coated magnetic nanoparticles after i.p. administration is above 2000 mg/kg [35]. Other studies in mice revealed that after i.p. administration LD_{50} for Fe_3O_4-composed and daunorubicin-loaded magnetic nanoparticles is 1010 mg/kg [36], and for Fe_3O_4-composed and Au-coated magnetic nanoparticles LD_{50} is 8390 mg/kg [37]. In our study, the i.p. administration of high doses of SPIONs-PAA resulted in their accumulation inside the phagocytes of the reticulo-endothelial system of spleen and liver. Histologically, no damages in the liver of low and high dose SPIONs-PAA-treated mice were detected because iron-induced hepatocellular injury does not occur when SPIONs are taken up by reticuloendothelial cells [38]. The i.p. administration of low doses of SPIONs-PAA as well as SPIONS-PAA-PEI-pDNA^{GFP} did not result in any alterations in the histological specimen (data not shown) as well as in the level of iron measured in the internal organs of mice. On the other hand, Trubetskoy *et al.* observed extensive parenchymal destruction of the mice liver after i.v. administration of complexes composed of PAA, PEI and pDNA, but without SPIONs, at slightly higher dose than ours [23]. This suggests that *in vivo* usage of our SPIONs-PAA-PEI-pDNA^{GFP} is safe when their mass ratio and dosage is carefully constructed.

Cellular uptake of SPIONs for magnetofection is the doorway for efficient nucleic acid delivery to the cell nucleus. It has been shown in many studies that malignant cells internalize more SPIONs than normal cells [34,39,40]. After 4-h incubation, we detected internalized SPIONs-PAA-PEI-pDNA^{GFP} at the mass ratio 0.6:1:1 in cells of all four cell lines, however, at that time no statistically significant differences in the internalization between normal and malignant cells were measured. On the other hand, after 24-h incubation, diverse GFP levels among the cell lines were determined: malignant mouse B16F1 and human SK-MEL-28 melanoma cells outperformed normal human mesothelial MeT-5A cells and mouse fibroblasts L929. After 24-h incubation, no SPIONs-PAA-PEI-pDNA^{GFP} inside the nuclei of B16F1 cells were detected, but we observed internalized SPIONs-PAA-PEI-pDNA^{GFP} in the endocytotic compartments with disrupted membranes, which indicates the infamous PEI-related proton sponge effect mechanism [41]. The direct evidence that PAA as an endosomolytic polymeric anion also contributed to the membrane disruption could not be observed, however, increased levels of GFP and IL-12 obtained after magnetofection of B16F1 cells with SPIONs-PAA-PEI in comparison to PEI is an indirect indication.

To further evaluate SPIONs-PAA-PEI as delivery systems for pDNA *in vitro* and *in vivo*, we first compared *in vitro* efficacy of magnetofection of mouse melanoma B16F1 cells with pDNA^{GFP} and pDNA^{IL-12} using SPIONs-PAA-PEI to the efficacy of transfection using PEI, 3 commercially available magnetic nanoparticles for magnetofection, electroporation, lipofection and SPIONs-PAA-PEI in the absence of an external magnetic field. PEI is well known transfection agent with pronounced endosomolytic properties [19], however, when coupled with SPIONs, synergistic effect in transfection efficacy has been observed [11,20,21]. Coating and functionalization of SPIONs with PAA and PEI, respectively, significantly increased magnetofection efficacy of mouse melanoma B16F1 cells with pDNA^{GFP} and pDNA^{IL-12} in comparison to the transfection using PEI only. Moreover, SPIONs-PAA-PEI outperformed all commercially available magnetic nanoparticles that we tested either at the percentage of GFP-positive cells or at the fluorescence intensity of GFP. Magnetofection efficacy of B16F1 cells with pDNA^{GFP} using SPIONs-PAA-PEI was about the same as that obtained by lipofection and electroporation. In another study transfection of B16F1 cells with pDNA^{GFP} using electroporation resulted in approx. 1.5-fold more GFP-positive cells that we observed after electroporation [42]. However, for more accurate evaluation of transfection efficacy also the fluorescence intensity of GFP, indicating the amount of the protein synthesized, should be taken into account. The amount of secreted IL-12 from B16F1 cells was statistically significantly higher after magnetofection than after transfection with PEI and lipofection. Cationic lipids efficiently deliver pDNA by endocytosis [43], and destabilize fluid lipid bilayers of cell membranes by promoting the formation of non-bilayer lipid structures [44]. Significantly lower amount of secreted IL-12 from B16F1 cells after lipofection in comparison to magnetofection and electroporation might indicate liposome-induced alterations in cell membrane resulting in diminished exocytosis-mediated protein secretion.

Magnetofection of tumors with pDNA^{GFP} using SPIONs-PAA-PEI was the first step in evaluating the efficacy of our gene delivery system also *in vivo*. To date, only two research groups report about efficient non-virally-associated magnetofection of tumors with pDNA encoding reporter gene with PEI-PEG-chitosan copolymer-coated magnetic nanoparticles or magnetic crystal-lipid nanostructure [45–47]. In our study, the effect of an external magnetic field on magnetofection of melanoma B16F1 and mammary adenocarcinoma TS/A tumors with pDNA^{GFP} using SPIONs-PAA-PEI was more pronounced in TS/A tumors than in B16F1 tumors. In the second step we evaluated the antitumor effectiveness of pDNA^{IL-12} after magnetofection with our SPIONs-PAA-PEI in weakly immunogenic TS/A mammary adenocarcinoma [29]. The therapeutic effect after magnetofection of TS/A tumors with pDNA^{IL-12} using SPIONs-PAA-PEI was significantly better than administration of SPIONs-PAA-PEI-pDNA^{IL-12} in the absence of an external magnetic field. In fact, there was no antitumor effect without the exposure of tumors to an external magnetic field. Interestingly, the contribution

of an external magnetic to the magnetofection efficacy was not seen *in vitro* but only *in vivo*. *In vitro*, internalization of SPIONS is usually limited by the lack of contact between SPIONs and cellular surface, and can be enhanced by increasing either gravitational or magnetic force. The gravitational force is a function of particle density and radius, and in standard *in vitro* conditions causes the sedimentation of SPIONs onto the cellular surface [48]. The gravitational force might have enabled 250 nm-sized SPIONs-PAA-PEI-pDNA^{GFP} and SPIONs-PAA-PEI-pDNA^{IL-12} to sediment onto the cellular surface during 4-h incubation, thus the exposure of cells to an external magnetic field could not additionally contribute to the sedimentation onto the cellular surface, subsequent internalization and nevertheless magnetofection of cells. *In vivo*, i.t. administration of SPIONs-PAA-PEI-pDNA^{IL-12} with subsequent exposure to an external magnetic field resulted in significant antitumor effect. The exposure of tumors to an external magnetic field after administration of SPIONs prolonged their retention at the targeted site [8,11,49], which might have contributed to the increased magnetofection efficacy of the magnet-exposed tumors. However, further studies are needed in order to elucidate the importance of an external magnetic field for the treatment of different tumors using magnetofection.

To the best of our knowledge, pDNA encoding therapeutic genes was delivered into tumors by magnetofection in only two studies by the same research group, dealing with dose-escalation neoadjuvant gene therapy of feline fibrosarcomas before surgery [14,16]. Magnetofection of fibrosarcomas turned out to be safe and efficient with the use of intermediate pDNA dose, which was explained by the bell-shaped dose dependence of IL-2 [50]. In our study, magnetofection of TS/A tumors with pDNA^{IL-12} resulted in significant antitumor effect as the only treatment modality. Furthermore, the effect of IL-12-based treatments of TS/A tumors after magnetofection was equal to the one of well-established and efficacious non-viral gene delivery methods *in vivo* – gene electrotransfer [27,51]. Three repetitive treatments with the same dosage of pDNA^{IL-12} resulted in the same significant antitumor effect. Magnetofection of tumors with pDNA^{IL-12} using SPIONs-PAA-PEI can be further refined for cancer immuno-gene therapy, which can be very efficient in combination with other treatment modalities, *e.g.* irradiation [52], particularly for the patients whose tumors cannot be removed by surgery [53].

5. Conclusion

The combination of coating and functionalization of SPIONs using PAA and PEI pH-responsive endosomolytic polymers as membrane disruptive agents proved to be nontoxic and effective for *in vitro* magnetofection of different cells with pDNA encoding either GFP or IL-12, and even superior in transfection efficacy than some other non-viral transfection approaches. *In vivo*, we demonstrated that magnetofection of mammary adenocarcinoma TS/A tumors with pDNA encoding IL-12 using SPIONs-PAA-PEI resulted in significant antitumor effect and could be further developed for cytokine-based tumor gene therapy.

Acknowledgement

We dedicate this work to A. Znidarsic, PhD, who passed away unexpectedly during the preparation of this manuscript. We sincerely acknowledge prof. J. Dolinsek, PhD, Josef Stefan Institute, Ljubljana, Slovenia, and prof. Z. Jaglicic, Institute of Mathematics, Physics and Mechanics, for facilitating us to do the measurements regarding the magnetic properties of our magnetic nanoparticles. We appreciate all the help by M. Lavric, B. Markelc, A. Sedlar and N. Rajnar that eased our work in achievement of our objectives. This work was financially supported by Slovenian Research Agency (program P3-0003, projects J3-2069, J3-4211) and conducted in the scope of the EBAM European Associated Laboratory (LEA) and COST Action TD1104.

References

[1] Mikhaylov G, Mikac U, Magaeva AA, Itin VI, Naiden EP, Psakhye I, et al. Ferri-liposomes as an MRI-visible drug-delivery system for targeting tumours and their microenvironment. Nat Nanotechnol 2011;6:594–602.
[2] Gupta AK, Gupta M. Synthesis and surface engineering of iron oxide nanoparticles for biomedical applications. Biomaterials 2005;26:3995–4021.
[3] Lin MM, Kim dK, El Haj AJ, Dobson J. Development of superparamagnetic iron oxide nanoparticles (SPIONS) for translation to clinical applications. IEEE Trans Nanobioscience 2008;7:298–305.
[4] Hofmann-Amtenbrink M, Hofmann H, Montet X. Superparamagnetic nanoparticles – a tool for early diagnostics. Swiss Med Wkly 2010;140:w13081.
[5] Sanchez-Antequera Y, Mykhaylyk O, van Til NP, Cengizeroglu A, de Jong JH, Huston MW, et al. Magselectofection: an integrated method of nanomagnetic separation and genetic modification of target cells. Blood 2011;117:e171–81.
[6] Chen B, Wu W, Wang X. Magnetic iron oxide nanoparticles for tumor-targeted therapy. Curr Cancer Drug Targets 2011;11:184–9.
[7] Prijic S, Sersa G. Magnetic nanoparticles as targeted delivery systems in oncology. Radiol Oncol 2011;45:1–16.
[8] Scherer F, Anton M, Schillinger U, Henke J, Bergemann C, Krüger A, et al. Magnetofection: enhancing and targeting gene delivery by magnetic force in vitro and in vivo. Gene Ther 2002;9:102–9.
[9] Plank C, Zelphati O, Mykhaylyk O. Magnetically enhanced nucleic acid delivery. Ten years of magnetofection-Progress and prospects. Adv Drug Deliv Rev 2011;63:1300–31.
[10] Krötz F, Sohn HY, Gloe T, Plank C, Pohl U. Magnetofection potentiates gene delivery to cultured endothelial cells. J Vasc Res 2003;40:425–34.
[11] Krötz F, de Wit C, Sohn HY, Zahler S, Gloe T, Pohl U, et al. Magnetofection–a highly efficient tool for antisense oligonucleotide delivery in vitro and in vivo. Mol Ther 2003;7:700–10.
[12] Kamau SW, Hassa PO, Steitz B, Petri-Fink A, Hofmann H, Hofmann-Amtenbrink M, et al. Enhancement of the efficiency of non-viral gene delivery by application of pulsed magnetic field. Nucleic Acids Res 2006;34:e40.
[13] Xenariou S, Griesenbach U, Ferrari S, Dean P, Scheule RK, Cheng SH, et al. Using magnetic forces to enhance non-viral gene transfer to airway epithelium in vivo. Gene Ther 2006;13:1545–52.
[14] Jahnke A, Hirschberger J, Fischer C, Brill T, Köstlin R, Plank C, et al. Intratumoral gene delivery of feIL-2, feIFN-gamma and feGM-CSF using magnetofection as a neoadjuvant treatment option for feline fibrosarcomas: a phase-I study. J Vet Med A Physiol Pathol Clin Med 2007;54:599–606.
[15] Lee CH, Kim EY, Jeon K, Tae JC, Lee KS, Kim YO, et al. Simple, efficient, and reproducible gene transfection of mouse embryonic stem cells by magnetofection. Stem Cells Dev 2008;17:133–41.
[16] Hüttinger C, Hirschberger J, Jahnke A, Köstlin R, Brill T, Plank C, et al. Neoadjuvant gene delivery of feline granulocyte-macrophage colony-stimulating factor using magnetofection for the treatment of feline fibrosarcomas: a phase I trial. J Gene Med 2008;10:655–67.
[17] Mykhaylyk O, Zelphati O, Hammerschmid E, Anton M, Rosenecker J, Plank C. Recent advances in magnetofection and its potential to deliver siRNAs in vitro. Methods Mol Biol 2009;487:111–46.
[18] Sapet C, Laurent N, de Chevigny A, Le Gourrierec L, Bertosio E, Zelphati O, et al. High transfection efficiency of neural stem cells with magnetofection. Biotechniques 2011;50:187–9.
[19] Boussif O, Lezoualc'h F, Zanta MA, Mergny MD, Scherman D, Demeneix B, et al. A versatile vector for gene and oligonucleotide transfer into cells in culture and in vivo: polyethylenimine. Proc Natl Acad Sci U S A 1995;92:7297–301.
[20] Wang XL, Zhou LZ, Ma YJ, Li X, Gu HC. Control of aggregate size of polyethyleneimine-coated magnetic nanoparticles for magnetofection. Nano Res 2009;2:365–72.
[21] Moghimi SM, Symonds P, Murray JC, Hunter AC, Debska G, Szewczyk A. A two-stage poly(ethylenimine)-mediated cytotoxicity: implications for gene transfer/therapy. Mol Ther 2005;11:990–5.
[22] Stayton PS, El-Sayed ME, Murthy N, Bulmus V, Lackey C, Cheung C, et al. 'Smart' delivery systems for biomolecular therapeutics. Orthod Craniofac Res 2005;8:219–25.
[23] Trubetskoy VS, Wong SC, Subbotin V, Budker VG, Loomis A, Hagstrom JE, et al. Recharging cationic DNA complexes with highly charged polyanions for in vitro and in vivo gene delivery. Gene Ther 2003;10:261–71.
[24] Massart R. Preparation of aqueous magnetic liquids in alkaline and acidic media. IEEE Trans Magn 1981;17:1247–8.
[25] Holzwarth U, Gibson N. The Scherrer equation versus the 'Debye-Scherrer equation'. Nat Nanotechnol 2011;6:534.
[26] Todorovic V, Sersa G, Mlakar V, Glavac D, Flisar K, Cemazar M. Metastatic potential of melanoma cells is not affected by electrochemotherapy. Melanoma Res 2011;21:196–205.
[27] Pavlin D, Cemazar M, Kamensek U, Tozon N, Pogacnik A, Sersa G. Local and systemic antitumor effect of intratumoral and peritumoral IL-12 electrogene therapy on murine sarcoma. Cancer Biol Ther 2009;8:2114–22.

[28] Bancroft J, Cook H. Manual of histological techniques and their diagnostic application. 1st ed. Edinburgh, New York: Churchill Livingstone; 1994.
[29] Rakhmilevich AL, Janssen K, Hao Z, Sondel PM, Yang NS. Interleukin-12 gene therapy of a weakly immunogenic mouse mammary carcinoma results in reduction of spontaneous lung metastases via a T-cell-independent mechanism. Cancer Gene Ther 2000;7:826–38.
[30] Cemazar M, Golzio M, Sersa G, Hojman P, Kranjc S, Mesojednik S, et al. Control by pulse parameters of DNA electrotransfer into solid tumors in mice. Gene Ther 2009;16:635–44.
[31] Cemazar M, Golzio M, Sersa G, Rols MP, Teissié J. Electrically-assisted nucleic acids delivery to tissues in vivo: where do we stand? Curr Pharm Des 2006; 12:3817–25.
[32] Li S, Zhang X, Xia X. Regression of tumor growth and induction of long-term antitumor memory by interleukin 12 electro-gene therapy. J Natl Cancer Inst 2002;94:762–8.
[33] Di Marco M, Sadun C, Port M, Guilbert I, Couvreur P, Dubernet C. Physicochemical characterization of ultrasmall superparamagnetic iron oxide particles (USPIO) for biomedical application as MRI contrast agents. Int J Nanomedicine 2007;2:609–22.
[34] Prijic S, Scancar J, Romih R, Cemazar M, Bregar VB, Znidarsic A, et al. Increased cellular uptake of biocompatible superparamagnetic iron oxide nanoparticles into malignant cells by an external magnetic field. J Membr Biol 2010;236: 167–79.
[35] Gajdosíková A, Gajdosík A, Koneracká M, Závisová V, Stvrtina S, Krchnárová V, et al. Acute toxicity of magnetic nanoparticles in mice. Neuro Endocrinol Lett 2006;27(Suppl. 2):96–9.
[36] Wu W, Chen B, Cheng J, Wang J, Xu W, Liu L, et al. Biocompatibility of Fe3O4/DNR magnetic nanoparticles in the treatment of hematologic malignancies. Int J Nanomedicine 2010;5:1079–84.
[37] Li Y, Liu J, Zhong Y, Zhang J, Wang Z, Wang L, et al. Biocompatibility of Fe3O4@Au composite magnetic nanoparticles in vitro and in vivo. Int J Nanomedicine 2011;6:2805–19.
[38] Bacon BR, Stark DD, Park CH, Saini S, Groman EV, Hahn PF, et al. Ferrite particles: a new magnetic resonance imaging contrast agent. Lack of acute or chronic hepatotoxicity after intravenous administration. J Lab Clin Med 1987; 110:164–71.
[39] Jordan A, Scholz R, Wust P, Schirra H, Thomas S, Schmidt H, et al. Endocytosis of dextran and silan-coated magnetite nanoparticles and the effect of intracellular hyperthermia on human mammary carcinoma cells in vitro. J Magnetism Magn Mater 1999;194:185–96.
[40] Ma YJ, Gu HC. Study on the endocytosis and the internalization mechanism of aminosilane-coated Fe3O4 nanoparticles in vitro. J Mater Sci Mater Med 2007; 18:2145–9.
[41] Godbey WT, Wu KK, Mikos AG. Tracking the intracellular path of poly(-ethylenimine)/DNA complexes for gene delivery. Proc Natl Acad Sci U S A 1999;96:5177–81.
[42] Cemazar M, Sersa G, Wilson J, Tozer GM, Hart SL, Grosel A, et al. Effective gene transfer to solid tumors using different nonviral gene delivery techniques: electroporation, liposomes, and integrin-targeted vector. Cancer Gene Ther 2002;9:399–406.
[43] Zuhorn IS, Hoekstra D. On the mechanism of cationic amphiphile-mediated transfection. To fuse or not to fuse: is that the question? J Membr Biol 2002;189:167–79.
[44] Hafez IM, Maurer N, Cullis PR. On the mechanism whereby cationic lipids promote intracellular delivery of polynucleic acids. Gene Ther 2001;8:1188–96.
[45] Namiki Y, Namiki T, Yoshida H, Ishii Y, Tsubota A, Koido S, et al. A novel magnetic crystal-lipid nanostructure for magnetically guided in vivo gene delivery. Nat Nanotechnol 2009;4:598–606.
[46] Kievit FM, Veiseh O, Bhattarai N, Fang C, Gunn JW, Lee D, et al. PEI-PEG-Chitosan copolymer coated iron oxide nanoparticles for safe gene delivery: synthesis, complexation, and transfection. Adv Funct Mater 2009;19: 2244–51.
[47] Kievit FM, Veiseh O, Fang C, Bhattarai N, Lee D, Ellenbogen RG, et al. Chlorotoxin labeled magnetic nanovectors for targeted gene delivery to glioma. ACS Nano 2010;4:4587–94.
[48] Luo D, Saltzman WM. Enhancement of transfection by physical concentration of DNA at the cell surface. Nat Biotechnol 2000;18:893–5.
[49] Chertok B, Moffat BA, David AE, Yu F, Bergemann C, Ross BD, et al. Iron oxide nanoparticles as a drug delivery vehicle for MRI monitored magnetic targeting of brain tumors. Biomaterials 2008;29:487–96.
[50] Schmidt W, Schweighoffer T, Herbst E, Maass G, Berger M, Schilcher F, et al. Cancer vaccines: the interleukin 2 dosage effect. Proc Natl Acad Sci U S A 1995;92:4711–4.
[51] Tevz G, Kranjc S, Cemazar M, Kamensek U, Coer A, Krzan M, et al. Controlled systemic release of interleukin-12 after gene electrotransfer to muscle for cancer gene therapy alone or in combination with ionizing radiation in murine sarcomas. J Gene Med 2009;11:1125–37.
[52] Kamensek U, Sersa G. Targeted gene therapy in radiotherapy. Radiol Oncol 2008;42:115–35.
[53] Plank C. Nanomedicine: Silence the target. Nat Nanotechnol 2009;4:544–5.